

# Temperature and humidity compensation in the determination of solvent vapors with a microsensor system

Jeongim Park<sup>a</sup> and Edward T. Zellers<sup>\*ab</sup>

<sup>a</sup> Department of Environmental Health Sciences, University of Michigan, Ann Arbor, MI 48109-202, USA

<sup>b</sup> Department of Chemistry, University of Michigan, Ann Arbor, MI 48109-2029, USA

Received 6th June 2000, Accepted 8th August 2000

First published as an Advance Article on the web 21st September 2000

Accounting for changes in temperature and ambient humidity is critical to the development of practical field vapor-monitoring instrumentation employing microfabricated sensor arrays. In this study, responses to six organic vapors were collected from two prototype field instruments over a range of ambient temperatures and relative humidities (RH). Each instrument contains an array of three unthermostated polymer-coated surface acoustic wave (SAW) resonators, a thermally desorbed adsorbent preconcentrator bed, a reversible pump and a small scrubber cartridge. Negligible changes in the vapor sensitivities with atmospheric RH were observed owing, in large part, to the temporal separation of co-adsorbed water from the organic vapor analytes upon thermal desorption of preconcentrated air samples. As a result, calibrations performed at one RH level could be used to determine vapors at any other RH without corrections using standard pattern recognition methods. Negative exponential temperature dependences that agreed reasonably well with those predicted from theory were observed for many of the vapor-sensor combinations. It was possible to select a subset of sensors with structurally diverse polymer coatings whose sensitivities to all six test vapors and selected binary vapor mixtures had similar temperature dependences. Thus, vapor recognition could be rendered independent of temperature and vapor quantification could be corrected for temperature with sufficient accuracy for most applications. The results indicate that active temperature control is not necessary and that temperature and RH compensation is achievable with a relatively simple microsensor system.

## Introduction

Arrays of polymer-coated surface acoustic wave (SAW) vapor sensors can provide selective determinations of organic vapors alone or in simple mixtures.<sup>1–5</sup> A number of studies have shown, however, that temperature and/or atmospheric water vapor can influence the performance of SAW sensors by causing shifts in the baselines and/or by altering responses to the targeted vapors.<sup>6–22</sup> These studies suggest that stand-alone vapor sensor arrays will have limited utility for environmental monitoring or for other applications subject to fluctuating ambient temperature and humidity, and that effective implementation of instrumentation employing sensor arrays will require ancillary components to compensate for such factors.

The effects of ambient temperature changes on SAW sensor array responses can be reduced by heat-sinking, insulating or actively controlling the array temperature (e.g., by use of a Peltier device).<sup>4,5,9,11,20</sup> Mixing the outputs of the working sensors with that from an unexposed reference sensor can reduce baseline drift, particularly if the reference sensor is coated with an interfacial polymer having thermal expansion properties similar to that on each working sensor.<sup>9,11,14–18</sup> Preconcentration of vapor samples on to an adsorbent bed followed by rapid thermal desorption can produce a sharp sample pulse whose magnitude is less affected by thermal baseline drift.<sup>10,11,23,24</sup> Applying theoretical or empirical correction factors can also be effective in addressing temperature effects.<sup>6,7,9</sup>

The effects of ambient relative humidity (RH) changes on sensor array responses can be reduced by the use of membrane inlets,<sup>21</sup> preconcentrators containing hydrophobic adsorbents<sup>4,10,11</sup> and/or Nafion tubing.<sup>12,13,21</sup> Nafion tubing can be used for non-polar vapor samples to remove or reduce water vapor in the sample stream. As with temperature, applying

correction factors may also be effective for RH compensation with polymer-coated SAW sensors.<sup>6,7</sup>

In this paper, we describe tests of two identical prototype instruments, each of which contains an array of three SAW vapor sensors and an adsorbent preconcentrator. The instruments were designed for monitoring worker exposures to mixtures of organic vapors in the occupational environment,<sup>1,4</sup> and they have also been applied to the determination of solvents and solvent mixtures permeating through chemical protective clothing.<sup>25</sup> To reduce power requirements, active temperature control was not incorporated into the instrument design. Abrupt temperature changes are buffered by mounting the sensors in contact with brass fixtures having relatively large thermal masses. In contrast to previous testing of these instruments, where ambient temperature and RH were held constant, here a focus was placed on the effects of these environmental variables on vapor recognition and quantification, and on approaches to compensate for their influence on instrument performance.

## Experimental

### Instrumentation

The two instruments, each measuring 13 × 18 × 5.5 cm and weighing 1.2 kg, were constructed by Microsensor Systems (Bowling Green, KY, USA) and have been described in detail elsewhere.<sup>1,4,25</sup> Fig. 1 shows the primary components of the analytical subsystem: an array of three polymer-coated SAW resonators operating at 250 MHz, an uncoated reference SAW sensor, a small adsorbent preconcentrator and microprocessor controlled pneumatic and heating systems for sample capture, transport and thermal desorption. The sensors are clamped on to

brass plates and then mounted on the sides of a brass cube containing machined ports and channels for housing the sensors and for exposing the sensors to vapor samples.

A miniature, reversible-flow, rotary-vane pump collects the air samples. The preconcentrator consists of a short, thin-walled stainless-steel tube packed with 20 mg of porous styrene-divinylbenzene copolymer beads (XUS43565.01, Dow Chemical, Midland, MI, USA)<sup>10</sup> and wrapped with an insulated NiCr-wire heater coil. A larger plastic tube packed with activated charcoal and Drierite provides 'zero air' during thermal desorption and analysis of captured vapor samples. An on-board microcomputer controls the pump, solenoid valve and preconcentrator heater and collects the output signals from the sensors at a rate of 1 Hz. Data are transmitted *via* an RS-232 port to an external computer for display and processing. Operation from an internal battery is possible, but for all the experiments described here a regulated dc power supply was used.

An air sample is first drawn into the instrument at 0.12 L min<sup>-1</sup> for 2 min. Although the incoming sample passes over the sensor array, the sensors are deactivated during this period to save power and to reduce drift due to self-heating (see below). Vapors are trapped on the downstream preconcentrator adsorbent. The direction of the rotary-vane pump is then reversed and air is drawn at 0.030 L min<sup>-1</sup> through the charcoal-Drierite bed and back-flushed through the system to purge >90% of the adsorbed water vapor from the preconcentrator adsorbent. The sensor array and preconcentrator heater are then activated and the desorbed vapor is passed over the sensor array on a background of clean, dry air, after which the preconcentrator is allowed to cool in preparation for the next sample. An entire sampling and measurement cycle requires 5.5 min.

### Test vapors and sensor coatings

For testing the effects of ambient RH, test atmospheres of toluene (TOL), trichloroethylene (TCE), dichloromethane (DCL), butan-2-one (MEK), propan-2-ol (IPA), and perchloroethylene (PCE) were generated at 25 °C and 25, 50, and 75% RH. For testing the effects of ambient temperature, test atmospheres of TOL, TCE, DCL, MEK, IPA and isoamyl acetate (IAA) were generated at 30% RH and 15, 25, and 30 °C. All solvents were obtained in >98% purity from Aldrich (Milwaukee, WI, USA) and were used as received.

Coatings of polyisobutylene (PIB), poly(diphenoxypyrophosphazine) (PDPP), polyepichlorohydrin (PECH), fluoropolyol (FPOL), triphenylmethylpolysiloxane (OV-25) and bis(cyanooxy) polysiloxane (OV-275) were selected on the basis of their structural diversity and demonstrated stability as thin films.<sup>1,4,26</sup> The polymers are either rubbery, amorphous solids

above their glass transition temperatures,  $T_g$ , (PIB, PDPP, PECH, FPOL) or viscous liquids (OV-25, OV-275). In response to anomalies in the response characteristics for certain vapors as a function of temperature (see below), the  $T_g$  of FPOL was determined by differential scanning calorimetry (DSC7, Perkin-Elmer, Norwalk, CT, USA). Each polymer was applied by airbrush as a solution in a volatile solvent. The frequency shift due to each coating ( $\Delta f_c$ ) and the approximate thickness have been reported.<sup>4</sup> Following the study of RH, sensors coated with PDPP and OV-25 were replaced owing to an electronic cross-talk problem that manifested itself in the responses from these two sensor tracking each other. These sensors had provided stable responses for more than 2 years prior to being replaced, and the cause of this problem was never determined. Values of  $\Delta f_c$  for the new sensors coated with PDPP and OV-25 were 429 and 343 kHz, respectively. Their previous values were 449 and 424 kHz, respectively.

### Data collection and analysis

Both instruments were placed in a thermostated chamber (Psychotherm G-27, New Brunswick Scientific, New Brunswick, NJ, USA). Test atmospheres were prepared in a series of 3 L Tedlar bags (SKC, Eighty Four, PA, USA) housed within the chamber and connected to the instruments *via* a manifold of Teflon solenoid valves (Neptune Research, Maplewood, NJ, USA). A flow-temperature-humidity controller (FTH, Model HCS 301, Miller-Nelson Research, Carmel Valley, CA, USA) provided dilution air during test-atmosphere generation and a continuous purge of the exposure chamber during testing. Temperature and humidity were monitored within the chamber just above the instruments with an NBS-traceable thermometer and a digital humidity sensor.

Duplicate calibrations were performed for each vapor at a given temperature and humidity condition over a ~25-fold concentration range bracketing the American Conference of Governmental Hygienists' Threshold Limit Value (ACGIH-TLV) (*i.e.*, from 0.2 to 5  $\times$  TLV).<sup>27</sup> The two instruments were tested in parallel. Vapor concentrations were corrected for temperature using the ideal gas law, where necessary, and were confirmed by an in-line GC-FID system equipped with a gas-sampling loop that was controlled by a computer running ChromPerfect software (Version 3.0, Justice Innovation, Palo Alto, CA, USA). Calibration curves were prepared by plotting the maximum frequency shift,  $\Delta f$  (Hz), *versus* concentration,  $c$  (g L<sup>-1</sup>), at five concentrations. Prior to each calibration a series of blank exposures were performed and the baseline from each sensor was measured. The sensitivity ( $\Delta f/\Delta c$ ) for each vapor-sensor combination was determined, after subtraction of the average baseline response, from the slope of the calibration curves by linear regression with forced zero.

Humidity levels considered in this study were constrained to 25–75% RH by the FTH controller. Air at <25% RH could not be generated reliably because the source was house air, which had a low and variable RH level, and because a finite portion of the air flow within the FTH passes over the internal water reservoir. At >75% RH, condensation of water vapor in the tubing became a problem because of back-pressure created between the controller and the solenoid valve assembly used to direct the air flow.

Practical limitations of the testing system also restricted the lowest temperature condition to 15 °C. The highest temperature planned for testing was 40 °C. However, at 40 °C, the sensor coated with PIB became unstable. The effect was reversible upon lowering the temperature and was probably due to excessive acoustic energy loss accompanying the approach of the coating-film resonance condition at this temperature.<sup>15</sup> Even at temperatures as low as 32 °C, vapor exposure led to cessation of oscillation, most likely for the same reason. In addition, non-

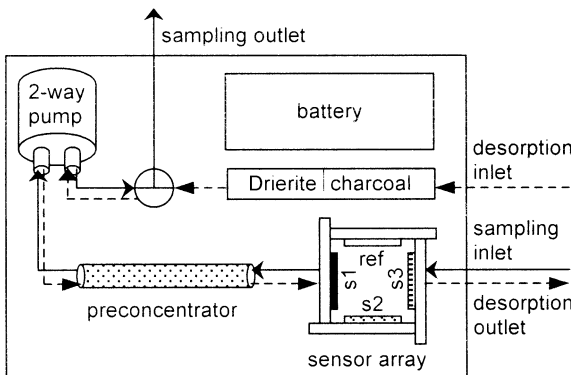


**Fig. 1** Diagram of the key instrument components showing sampling flow (—) and desorption flow (---) directions. s1, s2, and s3 are sensors coated with different polymers and ref is the reference sensor.

linearity in the responses to toluene were observed from the sensor coated with FPOL above 32 °C, which is unusual. As a result, the maximum chamber temperature was limited to 30 °C.

A fine-wire type-K thermocouple connected to a digital thermometer (Model HH-71 K1, Omega Engineering, Stamford, CT, USA) monitored the temperatures of one of the sensors in each of the two instruments. The thermocouple was placed on the three-pin header supporting the sensor and the leads were wedged between the sensor header and the wall of the brass cube. Since there is no active temperature control within the instruments, sensor temperatures varied with the chamber temperature. Heat generated by the instrument components raised the quiescent temperature of the sensors ~2 °C above ambient. Therefore, after a few initial cycles the actual baseline sensor temperatures were 17, 27 and 32 °C for the tests performed here. Upon activation of the sensors during the 60 s desorption/measurement period, a small additional increase of 0.5–0.6 °C due to self-heating occurred. This led to drift of the baseline frequencies of the sensors that ranged from ~300 to 1000 Hz. In spite of the magnitude of this drift, it was remarkably reproducible from run to run (RSD <2%), and accurate responses could be obtained after subtraction of the average baseline frequency determined prior to vapor exposures for each sensor. Repeated analyses of toluene over a 20 month period yielded sensitivities that varied by ≤7% (RSD) and showed no trends with time.

Following the individual vapor calibrations under the specified temperature and RH conditions, several additional exposure tests were performed with each vapor and with selected binary vapor mixtures at different temperatures. These response data were used as an independent test set for evaluating instrument performance. For the mixture analyses it was assumed on the basis of previous studies that the responses to the mixtures were linear combinations of the component vapor responses.<sup>1,4</sup> This permitted the use of individual-vapor calibrations in analyzing mixture responses in the test set.

Pattern recognition analyses were performed by extended disjoint principal components regression (EDPCR),<sup>28</sup> using

software routines written in-house in Visual Basic and run on a personal computer.

## Results and discussion

### Effect of ambient humidity on vapor responses

The effects of atmospheric humidity on the responses to the six organic vapors are summarized in Table 1. The calibration curves were linear ( $r^2 > 0.99$ ) over the vapor concentration ranges examined. As shown, there is little or no RH dependence of the sensor responses to the organic vapors. Owing to the relatively slow heating rate of the preconcentrator heater and the low affinity of the adsorbent for water vapor, the water vapor is separated chromatographically from even the most volatile (*i.e.*, earliest eluting) of the organic vapors, DCL. The response maximum for water vapor occurs at about 8 s after initiating the desorption step, whereas those for the organic vapors range from 15 to 26 s. Some overlap of the water-vapor tail occurs with the early-eluting vapor analytes (*i.e.*, DCL and MEK), but this is easily accounted for in the baseline subtraction step. Note that the dry-air purge step reduces the magnitude of the water-vapor response by over 10-fold and also reduces the variability of the response to the water vapor.<sup>4</sup> Without this step the water vapor response would obscure the DCL and MEK responses. Although it is theoretically possible to subtract the water vapor responses *via* pattern recognition,<sup>29</sup> in fact, the variability of the response (without the purge step) was too large to do this effectively.

The RSDs among the sensitivities at the three RH levels for a given vapor are all <10% and are typically <5%. A slight increase in sensitivity with increasing RH is observed for MEK and IPA with the first three sensors listed in Table 1, but this trend is not significant. None of the other sensor-vapor combinations show any discernable RH effect. Hence it can be concluded that neither the preconcentrator adsorbent nor the polymeric sensor coatings is affected by the presence of various

**Table 1** Comparison of vapor sensitivities at three different RH levels

Vapor	RH (%)	Sensitivity/Hz L $\mu\text{g}^{-1}$					
		PIB	PECH	PDPP	OV-275	OV-25	FPOL
TOL	25	10	7.8	4.6	3.4	8.6	2.4
	50	11	8.3	4.7	3.3	9.2	2.5
	75	9.9	7.9	4.7	3.5	8.5	2.4
	RSD (%)	5.9	3.3	1.2	2.9	4.3	2.4
	25	5.5	3.4	2.3	1.7	3.7	0.86
TCE	50	5.8	3.4	2.4	1.7	4.1	0.91
	75	5.4	3.3	2.3	1.6	3.8	0.94
	RSD (%)	3.7	1.7	2.5	3.5	5.4	4.5
	25	15	5.1	4.0	2.5	7.0	1.5
	50	14	5.0	4.2	2.3	6.5	1.4
PCE	75	14	5.1	4.3	2.4	6.7	1.5
	RSD (%)	4.0	1.1	3.7	4.2	3.7	3.9
	25	0.75	1.3	0.80	1.1	1.2	0.30
	50	0.77	1.4	0.82	1.1	1.4	0.26
	75	0.85	1.4	0.75	1.1	1.3	0.31
DCL	RSD (%)	7.4	4.2	4.6	0.0	7.7	9.1
	25	1.5	4.6	1.8	2.5	3.1	8.5
	50	1.6	4.8	1.7	2.5	3.1	8.7
	75	1.7	4.9	1.9	2.9	3.1	9.0
	RSD (%)	6.4	3.2	5.6	8.8	0.0	2.9
MEK	25	0.99	2.6	1.3	3.2	1.6	9.6
	50	1.1	2.9	1.2	3.1	1.5	10
	75	1.2	3.0	1.2	3.5	1.6	10
	RSD (%)	9.6	7.3	4.7	6.4	3.7	2.3
	25	0.041	0.12	0.068	0.45	0.27	0.15
Water	50	0.027	0.082	0.041	0.27	0.095	0.095
	75	0.068	0.082	0.14	0.26	0.068	0.082

amounts of water vapor over this range. It should be mentioned that the same adsorbent material was effective in preconcentrating vapors from exhaled breath at 100% RH in a similar sensor system configuration.<sup>10</sup>

It follows that there should be no significant difference among the relative response patterns measured under the three RH conditions, which means that there should be minimal impact on recognition rates for samples collected under ambient RH conditions that differ from those during calibration. This implies that calibrations need not control for RH. To investigate this, the series of 60 responses collected from the instruments at 25 or 75% RH were analyzed by EDPPCR using calibrations derived from responses collected at 50% RH. Table 2 shows the results of attempts to recognize and quantify the vapors in the test set using the three-sensor array consisting of sensors coated with PIB, PECH and OV-275. These three sensor coatings have been shown to provide excellent discrimination among different organic vapors.<sup>1,4</sup> Coincidentally, OV-275 is the most water-sensitive polymer among those tested here (Table 1). As shown in Table 2, vapors were correctly recognized in all 60 cases and the average quantification error was ~4% (range 0.1–9%).

Even with the dry-air purge step the *responses* to water vapor increase with increasing RH (Table 1). Note, however, that the *sensitivity* to water vapor generally decreases with increasing concentration. This behavior is consistent with expectations of a Langmuir-type adsorption isotherm for water vapor on the microporous adsorbent. The increase in water-vapor sensitivity observed at higher concentrations for PIB and PDPP may reflect non-linearity in the water-vapor sorption isotherms for these coatings, which are expected to increase in slope with

increasing concentration (*i.e.*, Type III sorption),<sup>6,9,30</sup> as well as adsorption of water vapor at the surface of the quartz sensor substrate, which can be significant for polar vapors with such non-polar sensor coatings.<sup>9,16,26,31</sup>

### Shifts in baseline with temperature

The baseline difference frequency for each sensor ranged from ~100 to 400 kHz and was fairly stable from day to day at a given temperature. Averages of >10 baseline measurements collected over several days at chamber temperatures of 15, 25 and 30 °C varied by <1% (RSD) for all six sensors. The baseline frequencies increased with increasing temperature owing to polymer thermal expansion.<sup>15,17,19,32</sup> Regressing these frequencies on to temperature over the range 15–30 °C gave linear relationships ( $r^2 > 0.91$ ), with slopes ranging from 470 to 1740 Hz °C<sup>-1</sup>. These are in reasonable agreement with those reported previously for the same or similar polymers,<sup>9,17,19</sup> although strictly they are not directly comparable owing to slight differences in the configurations employed and possible contributions from factors other than polymer thermal expansion.<sup>9</sup>

Comparison of these temperature coefficients with the vapor sensitivities in Table 1 shows that very small changes in temperature can cause significant errors in vapor determinations in the ppm range of concentration, as reported in earlier studies.<sup>9,12,13,17</sup> The reproducibility of responses obtained with these instruments attests to the utility of measuring pre-

**Table 2** Vapor recognition and quantification at 25 and 75% RH using calibration data generated at 50% RH from the array of three sensors coated with PIB, PECH and OV-275

25% RH					75% RH				
Vapor	Recognized as	Concentration/µg L <sup>-1</sup>			Vapor	Recognized as	Concentration/µg L <sup>-1</sup>		
		Actual	Predicted	Error (%)			Actual	Predicted	Error (%)
TOL	TOL	38	39	5	TOL	TOL	57	54	-4
	TOL	38	41	9		TOL	162	154	-5
	TOL	94	88	-6		TOL	377	378	0
	TOL	189	177	-6		TOL	943	943	0
	TOL	377	371	-2		TCE	134	130	-3
	TOL	943	926	-2		TCE	269	265	-1
TCE	TCE	54	53	-1		TCE	537	572	6
	TCE	54	57	7		TCE	1340	1390	4
	TCE	134	138	3		PCE	85	92	8
	TCE	269	256	-5		PCE	170	166	-2
	TCE	537	539	0		PCE	339	334	-1
	TCE	1340	1340	0		PCE	848	842	-1
PCE	PCE	51	54	5	MEK	MEK	236	237	0
	PCE	170	158	-7		MEK	590	571	-3
	PCE	339	324	-4		MEK	1180	1100	-7
	PCE	848	915	8		MEK	2780	2700	-3
MEK	MEK	59	61	3	DCL	DCL	243	238	-2
	MEK	59	55	-7		DCL	243	245	1
	MEK	177	187	6		DCL	347	364	5
	MEK	590	551	-7		DCL	347	357	3
DCL	MEK	1180	1210	3	IPA	DCL	562	578	3
	DCL	174	181	4		DCL	562	561	0
	DCL	174	185	7		DCL	1390	1340	-4
	DCL	347	354	2		IPA	123	126	3
IPA	DCL	694	689	-1		IPA	295	284	-4
	DCL	1390	1370	-1		IPA	566	590	4
	IPA	98	99	1		IPA	2950	3070	4
	IPA	98	100	2		IPA	4920	5080	3
	IPA	295	280	-5	Av. absolute quantification error (%)				
	IPA	583	559	-4	3				
	IPA	2950	2840	-4					
	IPA	4920	5010	2					
Av. absolute quantification error (%)					4				

concentrated samples over relatively short time periods to avoid longer term temperature induced baseline drift.

### Effect of temperature on vapor responses

It has been shown that the responses of polymer-coated SAW sensors to vapor sorption arise from roughly equal contributions from mass uptake and softening (*i.e.*, modulus reduction) of the polymer.<sup>33</sup> The latter has been attributed to the increase in free volume accompanying vapor sorption,<sup>15,34</sup> which is proportional to the mass of sorbed vapor. Hence the sensitivity is proportional to the vapor–polymer partition coefficient,  $K$ , which generally exhibits the following Arrhenius-type of temperature dependence:

$$\Delta f/\Delta C = \alpha K = K_0 e^{-\Delta H_s/RT} \quad (1)$$

where  $\alpha$  is an amplification factor accounting for the dependence of the SAW sensor response on modulus changes in the polymer,  $K_0$  is a temperature-independent pre-exponential factor,  $\Delta H_s$  is the heat of sorption,  $R$  is the gas constant and  $T$  is the absolute temperature.<sup>30</sup> The magnitude of the temperature dependence is a function of the heat of sorption, which is typically less than the heat of condensation because the process of mixing reduces slightly the heat generated by vapor partitioning into the polymer.<sup>9,30</sup>

Table 3 summarizes the observed effects of temperature on the vapor responses. The responses varied linearly with concentration at a given temperature, with  $r^2 > 0.99$  in all cases. The sensitivities decrease with increasing temperature, with the exception of combinations of TOL, DCL and TCE with FPOL. The anomalous decrease in sensitivity at lower temperatures for these vapors is unprecedented in our experience. Rebiere *et al.*<sup>8</sup> reported a slight decrease in the response of the chemical warfare agent GB with an FPOL-coated SAW sensor on reducing the sensor temperature from 35 to 30 °C. The FPOL used in their study was an isomerically pure 1,3-*trans* material with a reported  $T_g$  of ~35 °C. Although the response decrease in their case was small, one would have expected a fairly large *increase* in response over this temperature range. The FPOL we used is a mixture of isomeric forms having a  $T_g$  of 10 °C, as determined by differential scanning calorimetry. Thus, our results are in qualitative agreement with those of Rebiere *et al.* in the sense that responses diminish as the temperature is reduced toward the polymer  $T_g$ .

The decreased response at low temperature for the less polar vapors can be ascribed to a combination of slow diffusion associated with reduced polymer chain mobility as the temperature approaches  $T_g$  and the poor solubility of these vapors in FPOL. It is well known that vapors permeate films of FPOL relatively slowly at ambient temperatures.<sup>8,23</sup> However, if diffusion alone were responsible for the anomalous temperature

**Table 3** Effect of temperature on vapor sensitivities

Vapor	Temperature/°C <sup>a</sup>	Sensitivity/Hz L μg <sup>-1</sup>					
		PIB	PECH	PDPP	OV-275	OV-25	FPOL
TOL	15	16	13	6.9	5.2	15	1.2
	25	11	8.0	4.3	3.3	5.4	2.5
	30	8.2	6.1	3.6	2.8	2.6	2.6
	$r^{2b}$	0.994	0.999	0.995	0.995	0.990	0.917
	Temp. coeff. <sup>c</sup>	-4.3	-4.9	-4.4	-4.2	-11	5.3
	Ratio <sup>d</sup> (2.1) <sup>e</sup>	1.9	2.1	1.9	1.9	5.8	0.5
	15	9.1	5.2	3.6	3.4	6.8	0.60
TCE	25	5.9	3.3	1.9	1.7	2.2	0.91
	30	4.8	2.6	1.5	1.4	1.3	0.90
	$r^2$	1.000	1.000	0.994	0.992	1.000	0.897
	Temp. coeff.	-4.2	-4.5	-5.8	-6.0	-11	2.9
	Ratio (2.1) <sup>e</sup>	1.9	2.0	2.4	2.5	5.3	0.66
	15	1.2	2.2	1.2	1.8	2.6	0.16
	25	0.81	1.3	0.71	1.1	0.84	0.25
DCL	30	0.61	0.91	0.56	0.85	0.35	0.22
	$r^2$	0.993	0.991	1.000	1.000	0.983	0.663
	Temp. coeff.	-4.4	-5.5	-4.9	-4.9	-13	2.5
	Ratio (1.8) <sup>e</sup>	1.9	2.4	2.1	2.1	7.4	0.72
	15	2.4	6.2	2.8	10	3.2	28
	25	1.1	3.0	0.99	3.1	0.82	10
	30	0.76	1.9	0.71	2.1	0.35	6.0
IPA	$r^2$	1.000	0.997	0.993	0.993	0.995	1.000
	Temp. coeff.	-7.7	-7.7	-9.4	-11	-14	-10
	Ratio (3.0) <sup>e</sup>	3.2	3.2	4.0	4.8	9.0	4.7
	15	2.4	6.3	3.5	4.2	6.8	14
	25	1.6	4.4	2.2	2.5	2.3	8.5
	30	1.4	3.5	1.6	1.8	1.0	5.8
	$r^2$	0.977	0.995	0.988	0.996	0.983	0.987
MEK	Temp. coeff.	-3.9	-3.8	-4.9	-5.4	-11	-5.5
	Ratio (3.0) <sup>e</sup>	1.7	1.8	2.2	2.3	7.1	2.5
	15	36	36	26	10	43	55
	25	21	21	14	6.0	13	41
	30	13	15	8.5	4.0	6.0	31
	$r^2$	0.984	0.993	0.986	0.986	0.991	0.958
	Temp. coeff.	-6.4	-5.7	-7.1	-6.0	-13	-3.7
IAA	Ratio (2.6) <sup>e</sup>	2.7	2.4	3.0	2.6	7.2	1.8

<sup>a</sup> Test chamber temperature. <sup>b</sup> Regression  $r^2$  from plot of  $\ln(\text{sensitivity})$  vs.  $T^{-1}$ . <sup>c</sup> Rate of change in vapor sensitivity evaluated at 25 °C, % °C<sup>-1</sup>. <sup>d</sup> Ratio sensitivities at sensor temperatures of 17 and 32 °C (17:32 °C). <sup>e</sup> Theoretical sensitivity ratio (17:32 °C) calculated using the saturation vapor pressure under the assumption of ideal sorption behavior (see text).

dependence observed, then we should expect some consistency across all vapors. The greater degree of plasticization accompanying sorption of the more soluble vapors in the FPOL would facilitate diffusion into the film. The added reduction in the modulus of the FPOL for these vapors would further augment the SAW sensor response. Despite this odd temperature dependence, the isotherms even at low temperatures for TOL, DCL, and TCE were linear ( $r^2 > 0.99$ ).

To assess the magnitude of changes in sensitivities with temperature for the remaining vapor–polymer combinations, temperature coefficients were determined by evaluating the rate of the sensitivity change near 25 °C *via* eqn. (1). The temperature coefficients presented in Table 3 range from about  $-4$  to  $-14\text{ }^{\circ}\text{C}^{-1}$  over the range 15–30 °C. This means that the sensitivity will decrease at a rate of 4–14%  $\text{ }^{\circ}\text{C}^{-1}$ . The temperature coefficients for IPA are larger than those for the other vapors with all polymers, which is consistent with the larger heats of condensation of alcohols<sup>35</sup> and with a similar trend reported for butan-1-ol relative to other less polar vapors in some of the same sensor coating materials.<sup>9</sup>

Among the sensor coatings, OV-25 exhibits the largest temperature coefficient in all cases. A unique feature of this material was that the spray-deposited coating was not uniform or continuous but rather formed islands indicative of poor wetting and high surface tension.<sup>31,36</sup> This phenomenon was reported by Cai *et al.* for OV-25 on a flexural-plate wave sensor and it resulted in unstable sensor operation or loss of oscillation.<sup>23</sup> We found that the baseline had greater noise but that the response of the OV-25 coated sensor to vapors was fairly reliable.

Surface tension generally increases with decreasing temperature.<sup>37</sup> The enhanced temperature dependence for OV-25 may be attributable to this factor. We did not observe any unusual shifts in the baseline frequency of the OV-25 coated sensor upon cooling, but this source of interfacial stress between the polymer and the substrate would not be expected to contribute greatly to the baseline frequency,<sup>16,38</sup> particularly for a viscous liquid material such as OV-25. Subsequent vapor sorption, however, might reduce the surface tension and amplify the response relative to polymers where surface wetting was initially good and surface tension was low. Note that the temperature coefficients of sensitivity for OV-25 vary much less than those of the other coatings among the different vapors (Table 3). This indicates that whatever the enhancement mechanism, it dominates over the sorption thermodynamics represented by eqn. (1). Poor surface wetting has also been postulated as the cause of anomalous positive frequency shifts observed with SAW sensors coated with liquid crystals, where pre-treatment of the substrate with a methyl-terminated alkane-thiol was used to affect the liquid crystal alignment.<sup>39</sup>

As observed by Zellers and Han in their study of temperature effects on polymer-coated SAW sensor arrays,<sup>9</sup> several of the coatings have very similar temperature coefficients of sensitivity for a given vapor, whereas other coatings have different temperature coefficients. This will determine the extent to which response patterns will vary with temperature. Fig. 2 illustrates this point for TOL and TCE by presenting the relative response patterns for two different three-sensor arrays at 15, 25 and 30 °C. For the array in Fig. 2(a) and (b) the sensors have similar temperature coefficients and the response patterns of TOL and TCE do not change significantly with temperature. In Fig. 2(c) and (d), where coatings having very different temperature coefficients are included in the array, the response patterns change dramatically with temperature.

Selecting coatings for which the vapor sensitivities have similar temperature coefficients for a number of vapors appears possible. This, in turn, should provide a means of achieving independence from temperature in vapor recognition. The question that then arises is whether an array can be assembled with coatings having adequate structural diversity to recognize

and discriminate among all possible vapors and vapor mixture components of interest for a given situation.

To explore the performance of the instrument at different temperatures, an independent set of responses was collected at 15 and 30 °C and analyzed with the EDPCR. The sensitivities obtained previously for each vapor at 25 °C were used for calibration and an attempt was made to recognize and quantify the vapors on the basis of responses collected at the other temperatures. Table 4 shows the results using the array consisting of sensors coated with PIB, PECH and OV-275. As stated above, this array provides unique response patterns for a range of organic vapors.<sup>1,4</sup> From Table 3, this array is also expected to provide similar response patterns at the three temperatures for most of the six test vapors. Actually, in the cases of MEK and IAA, the array consisting of sensors coated with FPOL, OV-275 and PDPP will give more similar response patterns across this temperature range since their temperature coefficients are more similar than among other sensors, but this is not the case for the remaining vapors in the test set.

As shown in Table 4, the vapors were correctly recognized in all 48 individual vapor exposure tests. It must be appreciated that the response patterns for some of the vapors do change with temperature and, although these changes were not sufficient to cause confusion among this set of vapors, it is possible that with vapors giving more similar response patterns at the outset that increased recognition errors might be observed. It must also be appreciated that it is necessary to measure baseline frequencies at the temperature of measurement without any vapor present (*i.e.*, blank responses) and then to subtract these from the responses for the vapors. The accuracy of vapor recognition and quantification (see below) relies on this procedure.

For quantification, the theoretical correction factor reported by Zellers and Han was used.<sup>9</sup> Assuming ideal behavior, where the heat of sorption is equal to the heat of condensation, the vapor sensitivity should vary in proportion to  $T/P_{v(T)}$  where  $P_{v(T)}$  is the saturation vapor pressure at a given temperature.<sup>35</sup> That is, responses at  $T_1$  and  $T_2$  should differ by the factor  $(T_1/T_2)(P_{v(T_2)}/P_{v(T_1)})$ . The predicted ratio of sensitivities at sensor temperatures of 17 and 32 °C for each vapor is presented in Table 3 along with the measured ratios. With a few notable exceptions the agreement is fairly good, *i.e.*, within  $\sim 20\%$ . The ratios for OV-25 are larger than predicted for reasons explained above. Ratios for FPOL, even after excluding those for TOL, DCL and TCE, are not as accurately predicted in general. For the remaining four coated sensors only IPA and DCL have ratios that differ significantly from ideality, and only for one or two of the coated sensors. Note that the DCL ratios are all greater than predicted for the four well-behaved sensors. We

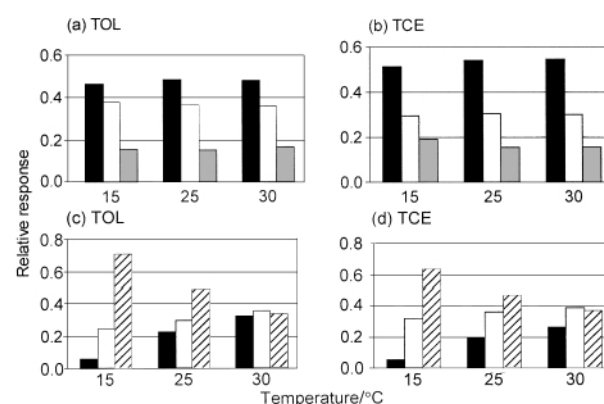


Fig. 2 Relative response patterns for toluene (TOL) and trichloroethylene (TCE) as a function of temperature for (a) and (b) the sensor array coated with PIB (■), PECH (□), and PDPP (▨), (c) and (d) the sensor array coated with FPOL (■), OV-275 (□), and OV-25 (▨).

cannot rule out the possibility that a fraction of the DCL vapor breaks through the adsorbent bed at the elevated temperatures, and that this contributes to the decrease in sensitivity with increasing temperature.

The data indicate that sensitivity changes can be predicted reasonably well from the temperature dependence of the vapor pressure of the analyte vapor. To test this, the theoretical correction factors were used to predict the sensor responses at chamber temperatures of 15 and 30 °C based on the responses measured at 25 °C. Using these predicted values to estimate the vapor concentrations by principal component regression yielded values that were within 8% on average of the actual values (Table 4). The errors for IPA at 15 °C are noticeably larger owing to the underestimate of the theoretical correction

for the OV-275 sensor. Overall there is a tendency toward underestimation, which can be attributed to the failure of the model to account for the slight positive temperature dependence of  $\alpha$  in eqn. 1, but the accuracy is adequate over these temperature ranges for most applications.

The problem of analyzing binary mixtures was then considered for two arbitrarily chosen vapor pairs, toluene + MEK and trichloroethylene + isoamyl acetate. For mixtures the recognition rate depends on the boundaries placed on the problem. If all possible combinations and subsets of six vapors are considered simultaneously, there are 63 possibilities. Evidence has been presented in a previous study suggesting that it is not possible to discriminate among such a large number of components with a polymer-coated sensor array, regardless of the size of the array (or the sensor technology employed).<sup>1</sup> However, an array of three sensors can often discriminate among the components of specified binary and ternary mixtures with high accuracy.<sup>1,4,23,25</sup> To evaluate the effect of temperature on the determination of mixtures with this prototype instrument, the same set of three coated sensors as used above was challenged with a binary mixture at two of the three test temperatures. Prior calibration data at 25 °C were used and responses obtained at the test temperatures were analyzed by EDPCR.

Table 5 shows that in six of the seven exposures at 15 or 30 °C, the mixtures were correctly differentiated from their individual vapor components. In the one errant case, TCE was not recognized when it was the minority component of the mixture with IAA at elevated temperature. All of the tests at 25 °C resulted in correct recognition of both components, as expected. Predicted concentrations showed more error than for the individual vapors, but were within 21% of the actual values in all cases. Hence the mixtures appear well-behaved and the data indicate that the sensor responses and physical properties of the individual vapors can be used to model the responses of simple mixtures as a function of temperature.

In summary, this study has demonstrated an effective approach to compensating for humidity and temperature effects in the determination of organic vapors with a field-deployable prototype instrument employing an array of microsensors. Compensation is achieved *via* a functionally integrated system comprising the sensor array, a vapor preconcentrator and a reversible sampling pump. Humidity effects are eliminated completely and temperature effects are easily addressed without active temperature control, such that calibrations need not account for changes in these variables. The practical implications of these results are significant. Although the ranges of humidity (25–75% RH) and temperature (15–30 °C) over which tests were performed were constrained, in part, by the test system, they span the ranges encountered in most indoor residential and working environments. Additional constraints on the effective temperature range of the instrument were imposed by thermally induced changes in the sensor coatings. Acoustic dampening associated with thin-film resonance effects, unusual variations in vapor sorption accompanying the onset of the polymer glass transition, and enhanced temperature sensitivity attributable to surface tension changes at the coating–substrate interface were apparent factors affecting the performance of several of the sensors as the operating temperature was varied.

## Acknowledgements

The authors are indebted to Chris Colburn of Sandia National Laboratories for fabricating the preconcentrator tubes used in the instrument, Brent Busey of Microsensor Systems for invaluable technical assistance, Meng-Da Hsieh for FPOL  $T_g$  measurements and Dr. Arthur Snow for providing a sample

**Table 4** Vapor recognition and quantification at chamber temperatures of 15 and 30 °C using calibrations generated at 25 °C from the array of three sensors coated with PIB, PECH and OV-275

Vapor	Temperature/°C	Recognized as	Concentration/μg L <sup>-1</sup>		
			Actual	Predicted <sup>a</sup>	Error (%) <sup>b</sup>
TOL	15	TOL	82	74	-9
	15	TOL	82	73	-11
	15	TOL	401	357	-11
	15	TOL	401	348	-13
	30	TOL	63	62	-2
	30	TOL	63	60	-5
	30	TOL	326	312	-4
	30	TOL	326	327	0
	15	TCE	122	126	3
	15	TCE	122	133	9
TCE	15	TCE	539	569	6
	15	TCE	539	569	5
	30	TCE	153	158	3
	30	TCE	153	151	-2
	30	TCE	486	455	-6
	30	TCE	486	489	1
	15	DCL	169	184	9
	15	DCL	169	188	11
	15	DCL	762	805	6
	15	DCL	762	786	3
DCL	30	DCL	283	258	-9
	30	DCL	283	247	-13
	30	DCL	714	601	-16
	30	DCL	714	637	-11
	15	IPA	280	348	24
	15	IPA	280	343	23
	15	IPA	2490	3010	21
	15	IPA	2490	3020	21
	30	IPA	297	282	-5
	30	IPA	297	267	-10
IPA	30	IPA	3060	2900	-5
	30	IPA	3060	2820	-8
	15	MEK	177	163	-8
	15	MEK	177	169	-4
	15	MEK	1240	1100	-11
	15	MEK	1240	1080	-13
	30	MEK	131	124	-5
	30	MEK	131	121	-7
	30	MEK	1090	1030	-6
	30	MEK	1090	1110	2
IAA	15	IAA	160	151	-6
	15	IAA	160	140	-12
	15	IAA	568	513	-10
	15	IAA	568	530	-7
	30	IAA	131	125	-4
	30	IAA	131	122	-7
	30	IAA	466	424	-9
	30	IAA	466	425	-9
	Av. absolute quantification error (%)		8		
	<sup>a</sup> Predicted concentration determined under the assumption of ideal behavior (see text). <sup>b</sup> 100 (predicted – actual)/actual.				

**Table 5** Recognition and quantification of binary vapor mixtures at different temperatures using individual vapor calibration data generated at 25 °C from the array of three sensors coated with PIB, PECH and OV-275

Vapor mixture	Temperature/°C	Recognized as	Concentration/ $\mu\text{g L}^{-1}$					
			Vapor a			Vapor b		
			Actual	Predicted <sup>a</sup>	Error (%)	Actual	Predicted <sup>a</sup>	Error (%)
TOL + MEK	15	TOL + MEK	70	57	-19	1600	1530	-4
TOL + MEK	15	TOL + MEK	207	175	-15	1240	1200	-3
TOL + MEK	15	TOL + MEK	382	334	-13	592	580	-2
TOL + MEK	15	TOL + MEK	402	370	-8	201	221	10
TOL + MEK	25	TOL + MEK	90	75	-17	552	603	9
TOL + MEK	25	TOL + MEK	192	204	6	572	536	-6
TOL + MEK	25	TOL + MEK	400	429	7	602	531	-12
TCE + IAA	25	TCE + IAA	279	274	-2	229	224	-2
TCE + IAA	25	TCE + IAA	521	444	-15	266	301	13
TCE + IAA	30	IAA	143	N/A <sup>b</sup>	—	503	483	-4
TCE + IAA	30	TCE + IAA	270	323	20	283	246	-13
TCE + IAA	30	TCE + IAA	518	418	-19	120	145	21

<sup>a</sup> Predicted concentration assuming ideal behavior. <sup>b</sup> Not assigned.

FPOL. Funding for this research was provided by Grant R01-OH03332 from the National Institute for Occupational Safety and Health of the Centers for Disease Control and Prevention.

## References

- 1 J. Park, W. A. Groves and E. T. Zellers, *Anal. Chem.*, 1999, **71**, 3877.
- 2 A. Hierlemann, U. Weimar, G. Kraus, M. Schweizer-Berberich and W. Gopel, *Sens. Actuators B*, 1995, **26–27**, 126.
- 3 J. Grate, S. J. Patrash, M. H. Abraham and C. M. Du, *Anal. Chem.*, 1996, **68**, 913.
- 4 J. Park, G.-Z. Zhang and E. T. Zellers, *Am. Ind. Hyg. Assoc. J.*, 2000, **61**, 192.
- 5 H. Wohltjen, D. S. Ballantine, Jr. and N. L. Jarvis, *ACS Symp. Ser.*, 1989, **403**, 157.
- 6 C. G. Fox and J. F. Alder, *Anal. Chim. Acta*, 1991, **248**, 337.
- 7 F. Benmakroha and J. F. Alder, *Anal. Chim. Acta*, 1995, **302**, 155.
- 8 D. Rebiere, C. Dejous, J. Pistre, J. Lipskier and R. Planade, *Sens. Actuators B*, 1998, **49**, 139.
- 9 E. T. Zellers and M. Han, *Anal. Chem.*, 1996, **68**, 2409.
- 10 W. A. Groves, E. T. Zellers and G. C. Frye, *Anal. Chim. Acta*, 1998, **371**, 131.
- 11 J. W. Grate, S. L. Rose-Pehrsson, D. L. Venezky, M. Klusty and H. Wohltjen, *Anal. Chem.*, 1993, **65**, 1868.
- 12 G. C. Frye, S. J. Martin, R. W. Cernosek and K. B. Pfeifer, *Int. J. Environ. Conscious Manuf.*, 1992, **1**, 37.
- 13 G. C. Frye and S. H. Pepper, *At-OnSite*, 1995, **1**, 62.
- 14 J. W. Grate, A. Snow, D. S. Ballantine, Jr., H. Wohltjen, M. H. Abraham, R. A. McGill and P. Sasson, *Anal. Chem.*, 1988, **60**, 869.
- 15 S. J. Martin, G. C. Frye and S. D. Senturia, *Anal. Chem.*, 1994, **66**, 2201.
- 16 J. W. Grate, M. Klusty, R. A. McGill, M. H. Abraham, G. Whiting and J. Andonian-Haftvan, *Anal. Chem.*, 1992, **64**, 610.
- 17 J. W. Grate, S. W. Wenzel and R. M. White, *Anal. Chem.*, 1992, **64**, 413.
- 18 Z. Liron, J. Greenblatt, G. Frishman, N. Gratziani and A. Biran, *Sens. Actuators B*, 1993, **12**, 115.
- 19 D. S. Ballantine, Jr. and H. Wohltjen, *ACS Symp. Ser.*, 1989, **403**, 222.
- 20 W. A. Groves and E. T. Zellers, *Am. Ind. Hyg. Assoc. J.*, 1996, **57**, 1103.
- 21 A. Kindlund, H. Sundgren and I. Lundstrom, *Sens. Actuators*, 1984, **6**, 1.
- 22 J. G. Brace, T. S. SanFelippo and S. G. Joshi, *Sens. Actuators*, 1988, **14**, 47.
- 23 Q. Y. Cai, J. Park, D. Heldsinger, M. D. Hsieh and E. T. Zellers, *Sens. Actuators B*, 2000, **62**, 121.
- 24 E. T. Zellers, M. Morishita and Q. Y. Cai, *Sens. Actuators B*, 2000, **67**, 244.
- 25 J. Park and E. T. Zellers, *J. Environ. Monit.*, 2000, **2**, 300.
- 26 S. J. Patrash and E. T. Zellers, *Anal. Chem.*, 1993, **65**, 2055.
- 27 American Conference of Governmental Industrial Hygienists (ACGIH), *2000 Threshold Limit Values for Chemical Substances and Physical Agents and Biological Exposure Indices*, ACGIH, Cincinnati, OH, 2000.
- 28 E. T. Zellers, S. A. Batterman, M. Han and S. J. Patrash, *Anal. Chem.*, 1995, **67**, 1092.
- 29 F. L. Dickert, O. Hayden and M. E. Zenkel, *Anal. Chem.*, 1999, **71**, 1338.
- 30 C. E. Rogers, in *Polymer Permeability*, ed. J. Comyn, Elsevier Applied Science, London, 1985, ch. 2.
- 31 R. A. McGill, J. W. Grate and M. R. Anderson, *ACS Symp. Ser.*, 1994, **561**, 280.
- 32 D. S. Ballantine, R. M. White, S. J. Martin, A. J. Ricco, E. T. Zellers, G. C. Frye and H. Wohltjen, *Acoustic Wave Sensors: Theory, Design, and Physicochemical Applications*, Academic Press, Boston, 1997.
- 33 J. W. Grate, S. N. Kaganove and V. R. Bhethanabolta, *Faraday Discuss. R. Soc. Chem.*, 1997, **107**, 259.
- 34 J. W. Grate and E. T. Zellers, *Anal. Chem.*, 2000, **72**, 2861.
- 35 R. J. Laub and R. L. Pecsok, *Physicochemical Applications of Gas Chromatography*, Wiley, New York, 1978, pp. 110–114.
- 36 J. W. Grate and R. A. McGill, *Anal. Chem.*, 1995, **67**, 4015.
- 37 A. W. Adamson, *Physical Chemistry of Surfaces*, Wiley, New York, 5th edn., 1990, pp. 54–56.
- 38 D. L. Bartley and D. D. Dominquez, *Anal. Chem.*, 1990, **62**, 1649.
- 39 E. T. Zellers, M. Oborny, R. Thomas, A. Ricco, G. C. Frye-Mason, G. Z. Zhang and C. Pugh, in *Proceedings of Eurosensors XIII, The Hague, Netherlands, September 16–19, 1999*, Delft University of Technology, Delft, The Netherlands, 1999, pp. 73–74.